

Spatiotemporal Structures and Mechanisms of the Tropospheric Biennial Oscillation in the Indo-Pacific Warm Ocean Regions*

TIM LI, PING LIU, X. FU, AND B. WANG

International Pacific Research Center, University of Hawaii at Manoa, Honolulu, Hawaii

GERALD A. MEEHL

National Center for Atmospheric Research,⁺ Boulder, Colorado

(Manuscript received 17 May 2005, in final form 1 September 2005)

ABSTRACT

The observed structure and seasonal evolution characteristics of the tropospheric biennial oscillation (TBO) in the warm ocean areas of the Indo-Pacific region are explored using a seasonal-sequence EOF analysis approach. The major convective activity centers associated with the TBO appear in the southeast Indian Ocean (SEIO) and western North Pacific (WNP), accompanied by anticyclonic (or cyclonic) circulation patterns with a first-baroclinic-mode structure. The convection and circulation anomalies have distinctive life cycles in the SEIO and WNP: the former have a peak phase in northern fall and the latter persist from northern winter to subsequent summer.

The mechanisms of the TBO in this region are investigated with a hybrid coupled GCM. Numerical results show that air–sea interaction in the warm ocean alone can support TBO variability that has many observed characteristics. Key processes involved in the TBO include the WNP monsoon variability and associated cross-equatorial flows, convective activity over Southeast Asia/the Maritime Continent and associated anomalous Walker circulation, and ocean dynamic responses to anomalous wind stress curl in the western Pacific. The coupled model experiment demonstrates that the essential element of the TBO in this region arises from the monsoon–warm ocean interaction.

A possible connection between the TBO and ENSO variability is further studied in another model that excludes the delayed oscillator dynamics. The key in causing the biennial variability of ENSO arises from teleconnections between the tropical Pacific and Indian Oceans, with three “atmospheric bridges”: 1) the north–south teleconnection that connects the WNP monsoon and the SEIO, 2) the east–west teleconnection that connects the Indian Ocean and the Pacific cold tongue, and 3) the El Niño–WNP monsoon teleconnection.

1. Introduction

The tendency of the south Asian monsoon rainfall anomaly to “flip-flop” in successive years is referred to as the tropospheric biennial oscillation (TBO; Meehl 1994, 1997). The TBO in monsoon rainfall has been

shown to depend critically on large-scale coupled air–sea interactions stretching from monsoon Asia to the eastern Pacific (Meehl 1987, 1994, 1997; Chang and Li 2000; Meehl and Arblaster 2002b; Meehl et al. 2003). Due to the large extent of the TBO, various observational studies have shown that the TBO is manifested over various monsoon regions such as Indonesia/northern Australia (Nicholls 1978; Yasunari and Suppiah 1988), East Asia/the western North Pacific (Lau and Sheu 1988; Masumoto and Yamagata 1991b; Tian and Yasunari 1992; Shen and Lau 1995; Chang et al. 2000ab; Wang and Li 2004; Li and Wang 2005), and India (Mooley and Parthasarathy 1984; Meehl 1987; Rasmusson et al. 1990; Yasunari 1990, 1991).

Among the many factors that influence the monsoon, El Niño–Southern Oscillation (ENSO) has been recognized as a major one (see a review by Webster et al.

* School of Ocean and Earth Science and Technology Contribution Number 6668 and International Pacific Research Center Contribution Number 382.

⁺ The National Center for Atmospheric Research is sponsored by the National Science Foundation.

Corresponding author address: Prof. Tim Li, IPRC and Dept. of Meteorology, University of Hawaii at Manoa, 2525 Correa Rd., Honolulu, HI 96822.
E-mail: timli@hawaii.edu

1998). The Indian monsoon in general tends to have a simultaneous negative correlation with the eastern Pacific SST (e.g., Rasmusson and Carpenter 1983; Shukla and Paolino 1983; Webster and Yang 1992; Yanai and Li 1994; Ju and Slingo 1995; Lau and Yang 1996; Yang and Lau 1998; Slingo and Annamalai 2000; Lau 2001) through connections involving the TBO (Meehl 1987, 1997). But this relationship is complex due to the involvement of the Indian Ocean (IO) SST anomaly (SSTA) (Lau and Nath 2000; Li and Zhang 2002; Li et al. 2005) and appears to have experienced an interdecadal change in the last several decades (Kumar et al. 1999; Chang et al. 2001).

The monsoon, on the other hand, may exert a strong feedback on El Niño (Masumoto and Yamagata 1991a; Wainer and Webster 1996) with the coupling between the Asia–Australia monsoon and tropical Pacific SSTs being an important part of the TBO (Meehl 1987, 1997). Chung and Nigam (1999) showed that the monsoon forcing might change the periodicity of El Niño. Kim and Lau (2001) demonstrated, in a simple model, that the monsoon forcing in the western Pacific might lead to a biennial tendency in the ENSO cycle.

While recognizing the interactive nature of the monsoon and ENSO, it is essential to understand the fundamental cause of the TBO. So far there are two schools of thought. One is that the TBO is originated in the tropical Pacific, as the delayed action oscillator may have an inherent biennial aspect, particularly when anomalous western Pacific winds associated with the Philippine Sea anticyclone are considered (Wang et al. 1999; Wang et al. 2000). The other view is that the Asian and Australian monsoons have an intrinsic biennial variability due to their interactions with adjacent warm oceans and the large-scale east–west circulation in the atmosphere (Meehl 1993, 1994, 1997; Chang and Li 2000; Li et al. 2001a,b) and as a result the biennial component of the ENSO has been connected to the monsoon forcing (Meehl 1987, 1997; Clarke and Shu 2000; Kim and Lau 2001; Chang and Li 2001).

The Asian–Australian monsoon and ENSO are characterized by both the TBO and lower-frequency (LF, 3–7 yr) components (Rasmusson et al. 1990; Barnett 1991; Ropelewski et al. 1992; Meehl 1997; Lau et al. 2000; Lau and Wu 2001). However, many current state-of-the-art coupled atmosphere–ocean GCMs fail to reproduce both the TBO and LF variabilities. For instance, the ECHAM–Hamburg Ocean Primitive Equation (HOPE) coupled GCM simulates a strong biennial ENSO but with a much weaker LF component (E. Roeckner 2004, personal communication), while the latest National Centers for Environmental Prediction (NCEP) coupled model generates very strong LF vari-

ability but very weak biennial variations (Wang et al. 2005). Issues to be resolved are why the two modes coexist in nature and what are fundamental processes that govern the TBO and LF variabilities. Previous studies suggest that the origin of the TBO and LF variabilities might be different. For instance, Zebiak and Cane (1987) showed that air–sea interactions in the tropical Pacific alone (without the involvement of the monsoon) could lead to the LF variability of ENSO. Meehl (1987, 1994, 1997), on the other hand, illustrated that the TBO represented the fundamental coupled processes of the monsoon–ENSO system, with El Niño and La Niña events being the extreme events in the TBO. Barnett (1991) noted that the near-equatorial characteristics of the TBO mode are those of a quasi-progressive wave while the characteristics of the LF mode are those of a standing wave. Li et al. (2001c) argued that the TBO variability involving Indian monsoon rainfall is primarily attributed to local processes over the tropical IO whereas the LF monsoon variability was attributed to remote forcing from the tropical Pacific Ocean.

The original seasonal evolution pattern of the TBO was provided by Meehl (1987), who described a distinct seasonal sequence for the TBO; that is, convection and circulation anomalies migrate southeastward from India in northern summer to northern Australia in northern winter as a natural enhancement or suppression of the climatological seasonal cycle of rainfall in those regions. However, the rainfall data used for this analysis were confined in the land and island stations and there were no data available over the oceans. Because of this limit, the seasonal evolution of the TBO is essentially along the “continental bridge” in that paper. Subsequently, atmosphere and ocean reanalyses, SST data, and global coupled climate model output have been analyzed to show the inherently large-scale coupled nature of processes in the Indo-Pacific region that combine to produce the TBO (Meehl 1993; Tomita and Yasunari 1996; Clarke et al. 1998; Ogasawara et al. 1999; Meehl and Arblaster 2002a; Loschnigg et al. 2003; Meehl et al. 2003).

The objective of this study is twofold. First, we intend to apply a season-sequence empirical orthogonal function (EOF) analysis approach to fully address the 3D TBO pattern and seasonal evolution characteristics. Second, with the aid of two different coupled atmosphere–ocean models, we intend to investigate the physical mechanisms, over the Indo-Pacific oceanic warm pool region, that are involved with the observed TBO evolution and structure. The outline of the rest of the paper is as follows. In section 2 we present results from a season-sequence EOF analysis to reveal funda-

mental features of the observed TBO. In sections 3 we analyze the TBO variability in a hybrid coupled GCM in which the atmosphere and ocean are fully interactive in the Indo-Pacific warm ocean region. A possible cause of the biennial variability of the ENSO is further studied in section 4. Finally, a conclusion is given in section 5.

2. Observed TBO structure and evolution characters

In this section we intend to address the dominant atmospheric circulation and convection patterns associated with the TBO and their seasonal evolution characters.

a. Data and bandpass filtering

The primary data used for this study are from the NCEP–National Center for Atmospheric Research (NCAR) reanalysis products from 1950 to 2003 (Kalnay et al. 1996). The monthly averaged data have a horizontal resolution of 2.5° latitude by 2.5° longitude and 12 pressure levels vertically. The 3D variables include the zonal and meridional wind components, vertical p velocity, and specific humidity. The monthly mean rainfall fields from the NCEP–NCAR reanalysis for 1950–2003 are used to represent large-scale convection. For the recent 25-yr (1979–2003) period, the reanalysis rainfall products have been validated against the Climate Prediction Center (CPC) Merged Analysis of Precipitation data (CMAP; Xie and Arkin 1997).

A sharp bandpass filter (Christiano and Fitzgerald 1999; see Fig. 1) was applied to the NCEP–NCAR reanalysis and the CMAP rainfall data to retain TBO

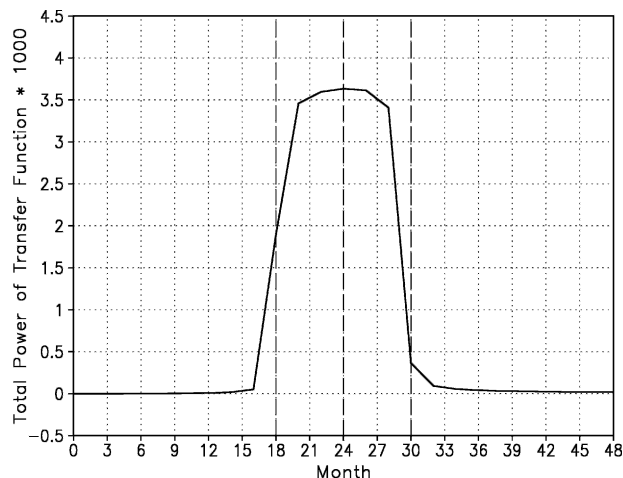


FIG. 1. A sharp bandpass filter with a period of 1.5–2.5 yr developed by Christiano and Fitzgerald (1999).

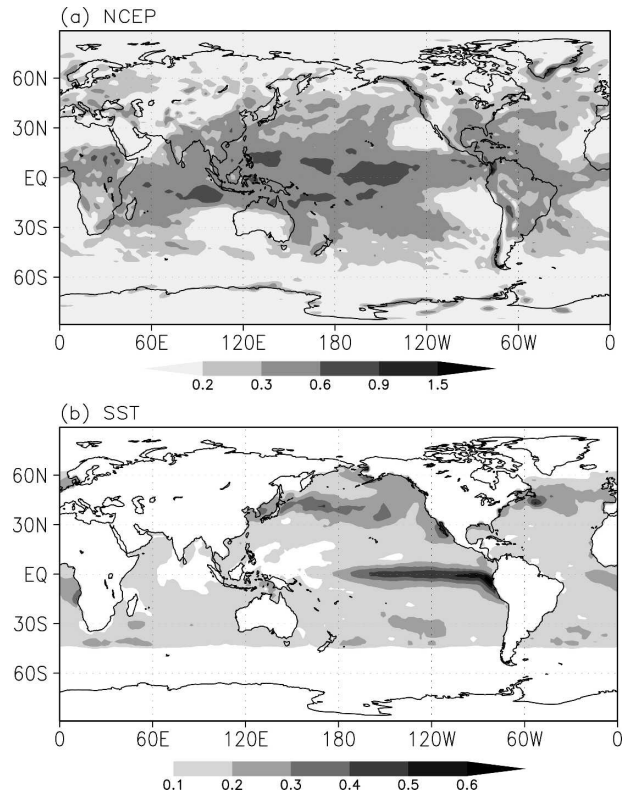


FIG. 2. Standard deviations of the quasi-biennial component of (a) rainfall (mm day^{-1}) and (b) SST (K) fields derived from the NCEP–NCAR reanalysis data.

(1.5–2.5 yr) signals. Figure 2a shows the standard deviation of the TBO bandpass-filtered rainfall fields from the NCEP–NCAR reanalysis. Compared to the CMAP products, the TBO rainfall variability derived from the reanalysis is a little (about 20%) weaker, but their spatial patterns are quite similar. In fact, their pattern correlation exceeds 0.7 in the global Tropics (30°S – 30°N). The result is consistent with Chen et al. (2004) who compared the two rainfall products in the East Asian summer monsoon domain. The fact that the major rainfall centers derived from the reanalysis are collocated with those from the CMAP data adds the confidence to use the reanalysis rainfall product for the TBO study for the entire period (1950–2003).

Figure 2a shows that the maximum convective activity centers associated with the TBO are located over the southeast Indian Ocean (SEIO) off Sumatra and the western North Pacific (WNP), whereas the rainfall variability in the Indian subcontinent is relatively weak. This points out that the greatest TBO convection centers in the monsoon region are located over the ocean, not over the land. Another maximum convective activity center resides in the central and eastern equatorial Pacific (CEP), which is closely related to the local SST

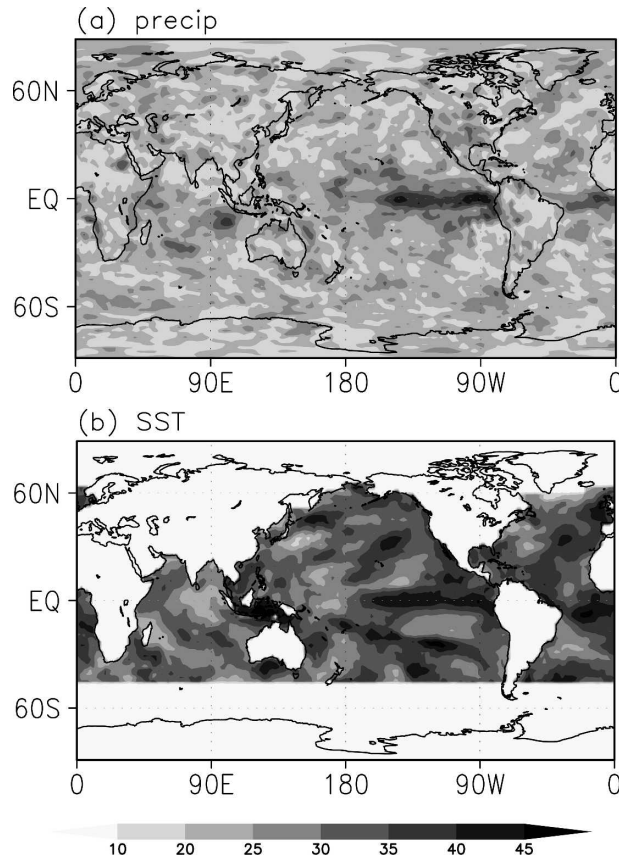


FIG. 3. Ratios (%) of standard deviations of quasi-biennial component of the total interannual component of the (a) precipitation and (b) SST fields.

variability there (Fig. 2b). In addition to its large amplitude in the equatorial eastern Pacific, SST also has significant biennial variabilities in the North Pacific and North Atlantic Oceans.

To illustrate the relative strength of the TBO, we calculated a ratio of the standard deviation of the TBO rainfall (or SST) field to that of the total interannual variability. (Here the total interannual anomaly is defined as a band of 1–8 yr.) It turns out that the ratio for the SSTA exceeds 35% over most of the tropical ocean region (Fig. 3). The TBO rainfall variability occupies a similar ratio in the SEIO and WNP, and so does the TBO variability of 850-mb zonal and meridional wind components (figure not shown).

b. A season-sequence EOF analysis

A conventional EOF analysis may depict spatial patterns of dominant modes, but it cannot provide a coherent seasonal evolution. To unravel seasonal-evolving TBO patterns, we apply a season-sequence

EOF (SSEOF) analysis, similar to that conducted by Wang et al. (2003). Here is a brief description of the SSEOF analysis. Suppose there are seasonal mean rainfall data in June–July–August of year 0 [JJA(0)], September–October–November of year 0 [SON(0)], December of year 0–January and February of year 1 [D(0)JF(1)], and March–April–May of year 1 [MAM(1)] over a spatial domain. The seasonal sequences over the entire domain are constructed into a large array, which is arranged along the rows of a large matrix, with time dimension (for different years) being in the columns. A conventional EOF is then applied to this reconstructed dataset. After the EOF, each summer-to-spring sequence shares the same time series but has different spatial patterns retrieved from the EOF. This SSEOF analysis was first applied to the filtered rainfall field, and then the time series of this first SSEOF mode is further regressed to other meteorological and oceanic variables.

We focus primarily on the warm ocean regions of the tropical Indian and western Pacific Oceans to elucidate the contribution to the TBO specifically from the coupled interactions in those regions. Figure 4 exhibits the seasonal evolution of the rainfall and 925-hPa wind anomalies associated with the TBO derived from the first SSEOF mode (at 15% of variance). (Here only the first half cycle of the TBO is plotted. The second half cycle is just a mirror image of the first one with an opposite sign.) The most pronounced feature in Fig. 4 is the evolution of two anomalous anticyclones and accompanying precipitation anomaly centers over the SEIO and WNP, respectively. During JJA(0), the low-level circulation anomalies are dominated by an elongated anticyclonic ridge extending from the Maritime Continent (MC) to India. Associated with this anticyclonic ridge is a tilted belt of pronounced anomalous westerlies extending from the Bay of Bengal (BOB) to the WNP, suppressed convection over the Maritime Continent, and enhanced convection over the Philippine Sea. Convection southwest of Sumatra is severely suppressed, which is associated with cross-equatorial flows west of Sumatra and a weak anticyclonic cell in the SEIO.

In SON, this SEIO anticyclone grows explosively, leading to a giant anticyclonic ridge that dominates the tropical IO and has its center at 10°S, 95°E. Intense easterly anomalies develop along the equatorial IO, and convection is suppressed in the SEIO while enhanced in the western IO—a typical dipole (or zonal) mode structure (Webster et al. 1999; Saji et al. 1999) that was shown earlier to be part of the TBO (Loschnigg et al. 2003; Meehl et al. 2003). Easterly anomalies and drought develop over the Maritime Con-

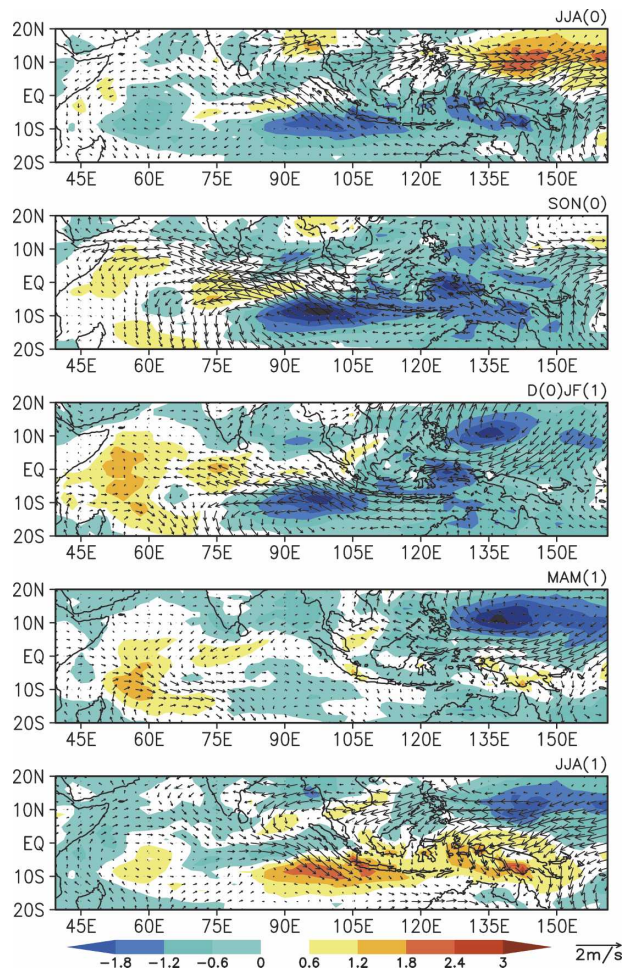


FIG. 4. Seasonal sequence of the rainfall anomaly (color shaded; mm day^{-1}) and 925-hPa wind anomaly (vector) associated with a half cycle of the TBO obtained from a SSEOF analysis using the NCEP–NCAR reanalysis data for 1950–2003.

continent and north of Australia. A weak anomalous low-level anticyclone forms west of the Philippines.

In DJF, the low-level circulation anomalies are dominated by two subtropical anticyclones located in the SEIO and the WNP, respectively. The former is a result of the weakening of the SEIO anticyclone from boreal fall, while the latter results from the amplification and eastward migration of the Philippine anticyclone (Wang and Zhang 2002).

In MAM there is a similar anomaly pattern in the WNP, characterized by the pronounced WNP anomalous anticyclone. The intensity of the WNP anticyclone however, decreases toward summer. By then, the SEIO anticyclone has completely disappeared.

During JJA(1), subsidence controls the Philippine Sea, signifying a weakening of the summer monsoon over the WNP. The anomaly pattern is opposite to the

one in the previous summer; that is, anomalous northwesterly and enhanced convection patterns appear in the SEIO while the suppressed convection and anomalous anticyclone occur in the WNP.

The two anomalous anticyclones in the SEIO and WNP have distinctive evolution characteristics. While the SEIO anticyclone is initiated in northern summer and peaks in northern fall, the WNP anticyclone is initiated in northern fall and persists from northern winter to the following summer. The distinctive evolution characteristics arise from differences in the basic-state wind between the two regions as air–sea interactions crucially depend on the annual cycle of the background flow (for detailed discussions see Wang et al. 2003; Li et al. 2003). We assume initially there is a weak cold SSTA off Sumatra in the boreal summer. Since the SEIO is a region with intense convection, the cold SSTA implies the reduction of atmospheric convective heating or an atmospheric heat sink. According to Gill's (1980) solution, the heat sink will induce a descending Rossby wave response to its west, resulting in an anomalous low-level anticyclone. In northern summer, the mean flow is southeasterly off Sumatra. Thus, the anomalous wind increases the total wind speed and cools the SST through enhanced surface evaporation, vertical mixing, and coastal upwelling. Through this positive thermodynamic air–sea (TAS) feedback (Wang et al. 2000), the cold SSTA develops. This feedback is most efficient in boreal summer when the mean flow is southeasterly (Li et al. 2003). When the background flow changes from southeasterly in summer to northwesterly in winter, the same anomalous wind would reduce total wind speeds and thus damp the original SSTA. This has been shown to be important for SST anomalies connected to Australian monsoon rainfall to the northwest of Australia (Hendon 2003). Thus, this mechanism acts as a negative feedback in northern winter. Because of its strong seasonal dependence, this feedback mechanism explains the rapid development of the circulation and SST anomalies off Sumatra in boreal summer and their turnabout in northern fall. On the other hand, the basic flow in the WNP is in a stable trade wind regime from northern winter to early summer. Thus, the difference in the basic flow accounts for the distinctive life cycles of the SEIO and WNP anticyclones.

Figure 5 shows the regressed circulation patterns at 200 mb. The structure of the upper-tropospheric circulation is to a large extent a mirror image with an opposite sign relative to the low-level circulation. Thus, the TBO in the monsoon region is dominated by a first-baroclinic-mode vertical structure.

Corresponding to a suppressed convective phase in the SEIO from JJA(0) to DJF(1), a positive SSTA de-

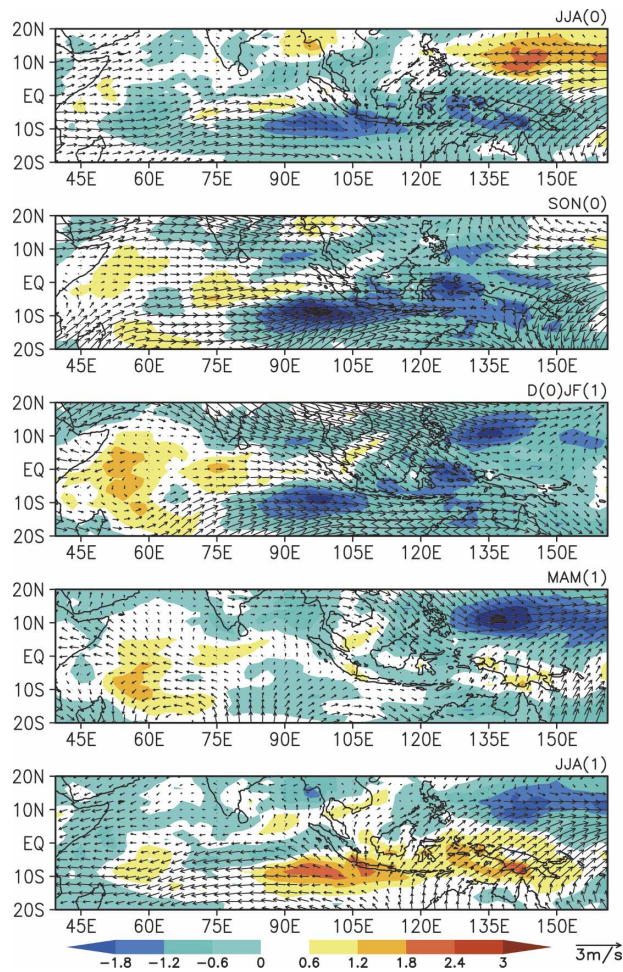


FIG. 5. Same as in Fig. 4, except for wind anomaly at 200 hPa (vector).

velops in the CEP (see Fig. 6). Note that the peak of the SSTA occurs in northern fall, which is one season earlier than the El Niño mature phase (DJF). The maximum SSTA center migrates westward along the equatorial Pacific. In the SEIO, a cold SSTA collocates with a negative rainfall anomaly and southeasterly wind anomaly during northern summer and fall. This phase relationship supports the positive air–sea feedback hypothesis elucidated by Li et al. (2003) and Wang et al. (2003). The SSTA off of Sumatra can be initiated by anomalous southeasterlies in situ, and the latter may be caused by the strengthening of the WNP monsoon (Li et al. 2002) or remote SSTA forcing from the CEP (Chamber et al. 1999; Reason et al. 2000).

3. Role of atmosphere–warm ocean interaction in the TBO

To address in more detail how ocean–atmosphere interactions in the warm ocean lead to the TBO, we rely

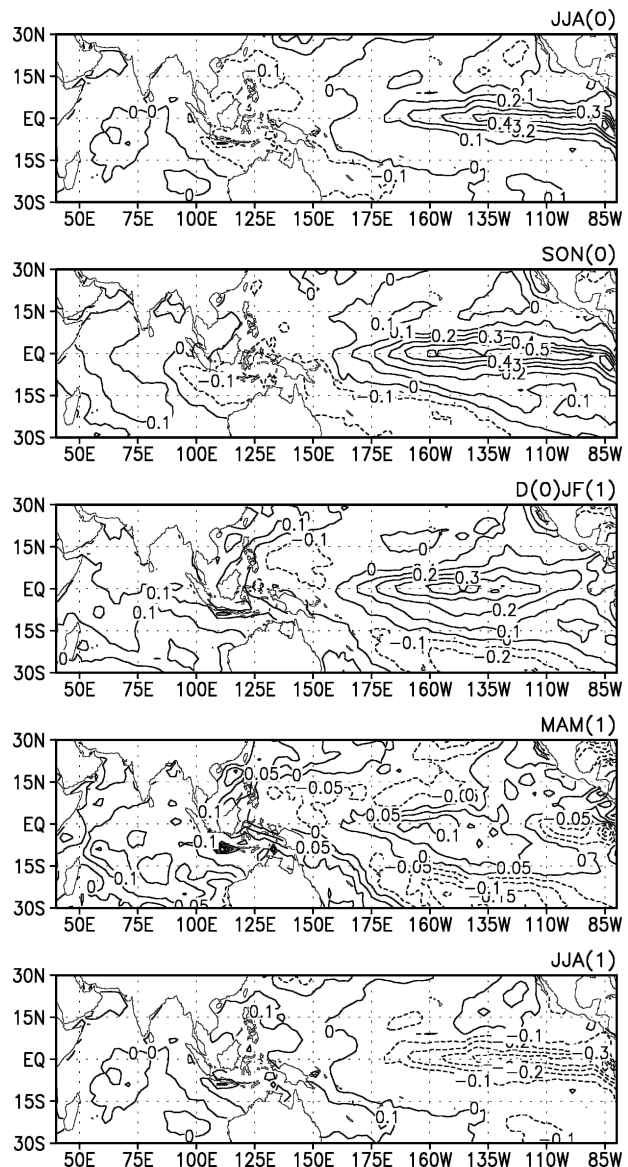


FIG. 6. Evolution of the quasi-biennial SSTA field (K) associated with the TBO.

on the diagnosis of idealized numerical experiments from a hybrid coupled atmosphere–ocean GCM in which the atmosphere and ocean are fully interactive only in the tropical IO and western Pacific.

a. The model and simulated mean climate

The atmospheric component of this hybrid coupled model is the ECHAM4 AGCM developed by the Max Planck Institute for Meteorology in Germany (for a detailed description, see Roeckner et al. 1996). The model dynamics is computed at a triangular truncation

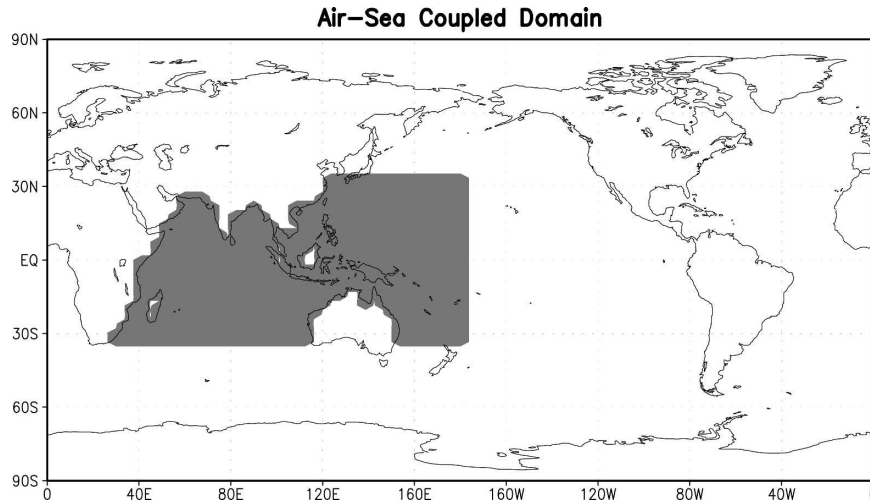


FIG. 7. The active air-sea interaction domain in the hybrid coupled GCM.

at wavenumber 30, while the physical parameterizations are calculated on the associated Gaussian grid. The model contains 19 layers extending from the surface to 10 hPa. The *mass flux scheme* for deep, shallow, and midlevel convection (Tiedtke 1989) was modified with respect to the closure for penetrative convection and the formation of organized entrainment and detrainment (Nordeng 1996). The deep convection closure depends on convective instability (CAPE) rather than the moisture convergence of Tiedtke (1989). The *radiation scheme* is a modified version of the European Centre for Medium-Range Weather Forecasts (ECMWF) scheme (Fouquart and Bonnel 1989; Morcrette et al. 1986). The single-scattering properties of cloud water droplets and ice crystals are parameterized according to Rockel et al. (1991). The *land surface scheme* is a modified bucket model (Dumenil and Todini 1992) with improved parameterization of rainfall-runoff. *Surface fluxes* of momentum, heat, water vapor, and cloud water are based on the Monin-Obukhov similarity theory (Louis 1979). The vertical diffusion in the model is computed with a high-order closure scheme depending on the turbulent kinetic energy (Brinkop and Roeckner 1995).

The ECHAM4 has been coupled to an intermediate ocean model without a heat flux correction (e.g., Fu et al. 2002, 2003). The intermediate ocean model consists of two active layers of the upper ocean, a mixed layer with variable depth, and a thermocline layer overlying an inert deep ocean (Wang et al. 1995). The latest version of the model combines the upper-ocean dynamics described in McCreary and Yu (1992) and the mixed layer physics (Gaspar 1988). The model has a self-contained parameterization scheme for the entrained

water temperature that considers the influences on the entrained water temperature from both the thermocline displacement and the mixed layer temperature (Wang et al. 1995). The effects of shear production, wind stirring, and buoyancy forcing are included in the vertical entrainment velocity calculation. The model has the capability of simulating a realistic annual cycle and interannual variations of SST, thermocline depth, and mixed layer depth (Fu and Wang 2001).

To explore the role of the atmosphere-warm ocean interaction, we designed an idealized hybrid coupled GCM experiment in which the atmosphere and ocean are coupled only in the tropical IO and western Pacific (30°S–30°N, 40°E–180°) while the climatological monthly mean SST is specified elsewhere. By doing so, we exclude the effects of the remote El Niño forcing. Figure 7 presents the coupled model domain.

To ensure a smooth transition in the model lateral boundaries, we set up a 5° transition zone at the north and south boundaries (at 30°S and 30°N) and a 10° transition zone at the eastern boundary at 180°. SSTs in the transition zones are a combination of the predicted and specified climatological monthly mean values. The ocean dynamic fields (e.g., u - v currents) are allowed to evolve freely across 180°.

After an initial 10-yr spinup, the coupled model was integrated for 50 yr. Figure 8 shows the summer and winter mean precipitation/low-level wind fields and SST errors. The seasonal mean SST errors are in general smaller than 1°C in most of the ocean domain except near the coast of North Africa in boreal summer and the coast of western Australia and the South China Sea (SCS) in boreal winter. The large error in the western Indian Ocean near the African coast is possibly

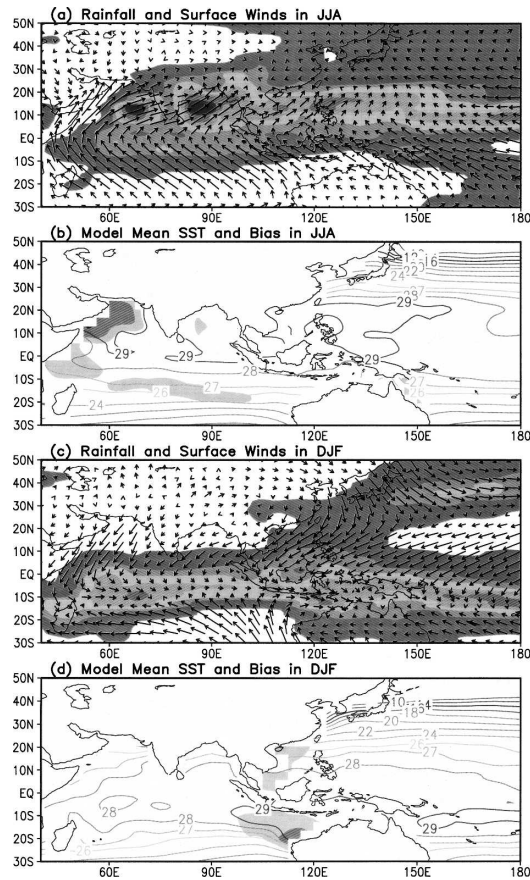


FIG. 8. Simulated seasonal mean rainfall and surface wind fields, mean SST (contour), and SST bias (shading) in (top) JJA and (bottom) DJF from the hybrid coupled GCM.

attributed to a too deep thermocline in the model, which underestimates coastal upwelling.

b. TBO variability in the model

Figure 9 illustrates the standard deviation of the total interannual (1–8 yr) variability of the model SST and the relative strength of the TBO (1.5–2.5 yr) component. (The same bandpass filtering and SSEO analysis method were applied here.) Note that the greatest interannual SST variabilities appear in the BOB, SEIO, WNP, and the South Pacific convergence zone (SPCZ), where the biennial component is also largest. The averaged ratio of the biennial SST variability in the four regions exceeds 60%, about a factor of 2 larger than what is observed in Fig. 3b, indicating that in this model configuration without the eastern tropical Pacific, the TBO is a dominant signal. Strong TBO signals also appear in the middle-tropospheric (500 mb) vertical motion and low-level (850 mb) zonal and meridional wind components. Figure 10 shows the power spectrums of the time series of the model SST and 500-mb

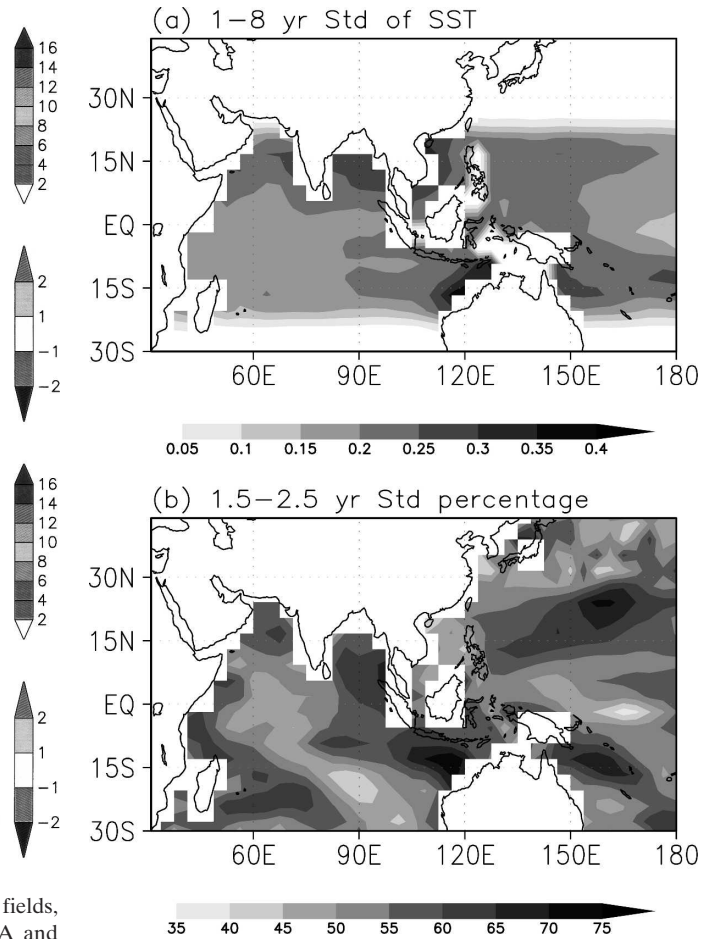


FIG. 9. (top) Standard deviation of the interannual (1–8 yr) SST variability (K) and (bottom) the ratio of the standard deviation of the quasi-biennial (1.5–2.5 yr) SST variability relative to the total interannual variability (%) derived from the hybrid coupled GCM.

vertical velocity over these regions. The TBO peaks, ranging from the period of 20 to 28 m, clearly appear in these spectrums, and they exceed a 95% significance level. The results above suggest that the monsoon–warm ocean interaction favors a pronounced biennial variability.

To illustrate the spatial pattern and evolution characteristics of the model TBO in the Indo-Pacific warm ocean region, we conducted the same SSEO analysis as in section 2, but with the use of the model data (and with a similar domain size). Figure 11 illustrates the seasonal evolution of 850-mb wind and 500-mb vertical p -velocity fields. (To better compare to Fig. 4, here the vertical velocity has been multiplied by -1 so that a positive value in Fig. 11 represents an enhanced rainfall anomaly.) Comparing Fig. 11 to Fig. 4, one may note that the model in general captures the gross structure

SST Power Spectra

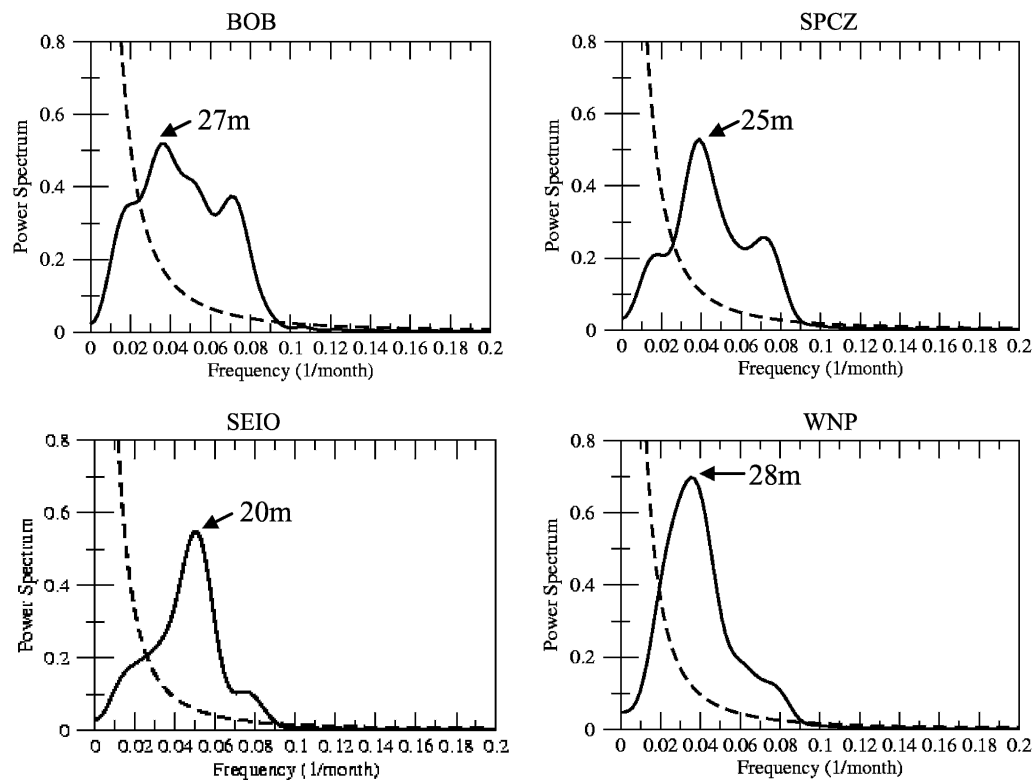
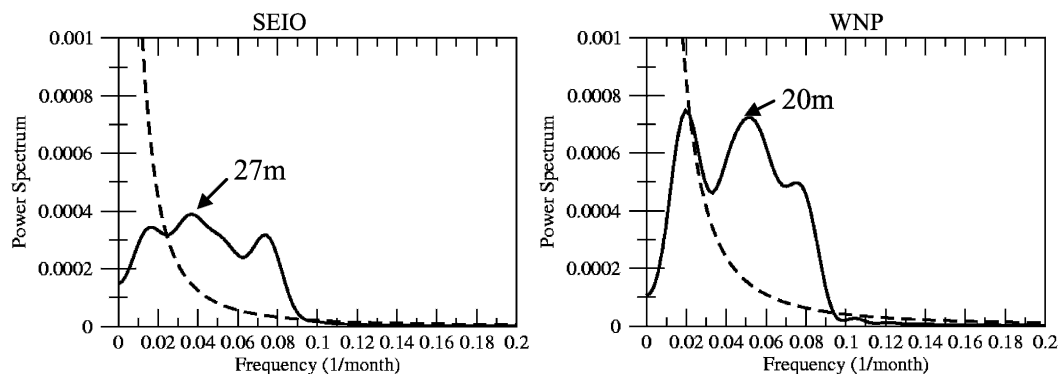
 ω Power Spectra

FIG. 10. (top, middle) Power spectra of the model interannual SST anomalies in the BOB, SPCZ, SEIO, and WNP, and (bottom) power spectra of 500-hPa vertical motion fields over the SEIO and WNP. The dashed line represents a 95% significance level. A dominant period is indicated in each panel.

and evolution patterns of the observed TBO in this region. For instance, in JJA(0), the circulation anomaly in the SEIO is characterized by downward motion (or suppressed convection) and anticyclonic low-level flows, while in the WNP it is characterized by cyclonic flows and upward motion. The SEIO anticyclone is pronounced in northern fall, and decays in subsequent seasons. Subsidence motion and anticyclonic flows develop over the Philippines and SCS in SON(0), and they shift

slightly eastward in subsequent seasons and persist until JJA(1). The circulation anomalies in JJA(1) have an opposite polarity relative to those in the previous summer.

c. TBO mechanisms in the Indo-Pacific warm ocean region

Since there is no SSTA forcing from the eastern Pacific, the model TBO arises from air–sea interactions in

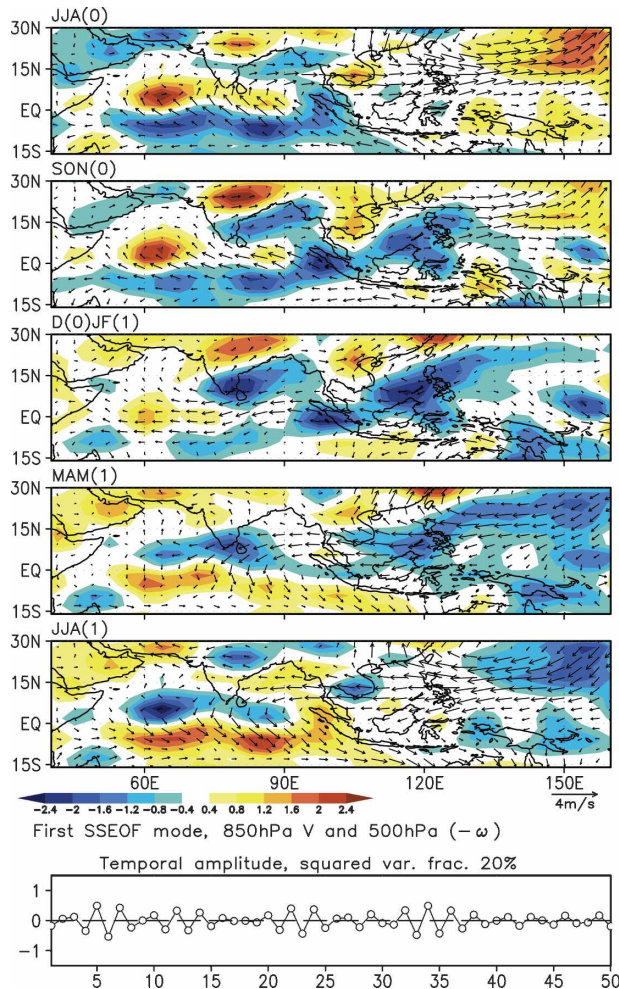


FIG. 11. Seasonal evolution of the 500-hPa vertical p velocity (color shaded; Pa s^{-1}) and 850-hPa wind anomaly (vector) associated with the TBO obtained from an SSEOF analysis of 50-yr output of the hybrid coupled GCM. (bottom) The time coefficient of the SSEOF mode. The vertical velocity has been multiplied by -1 so that positive contours represent enhanced convection anomalies.

the Indo-Pacific warm ocean region. A natural question is what are specific processes that give rise to the TBO variability in this region.

Figure 12 illustrates the seasonal evolution pattern of the SSTA, which is regressed based on the time coefficient of the first SSEOF mode. A significant surface cooling occurs in JJA(0) in the eastern IO and off the Asian coast, with maximum cold SSTA appearing in the BOB and SCS. While the cold SSTA decays in subsequent seasons, new cold SST anomalies develop in the western Pacific in SON(0) and DJF(1). In particular, the cold SSTA in the WNP reaches a peak in DJF(1) and persists for two to three seasons till the following summer, JJA(1), when the SSTA in the east-

ern IO and SCS has completely reversed sign from a cold to a warm anomaly.

The diagnosis of the model SST budget reveals that the cooling in the IO in JJA(0) is primarily attributed to the surface evaporation and vertical ocean mixing due to enhanced surface wind speeds, whereas the cooling in the western Pacific in SON(0) and DJF(1) is mainly attributed to the ocean dynamic processes in response to an anomalous wind stress curl (see discussions below). Based on the model circulation and SST evolution, a hypothesis is put forth to explain the TBO in the model. We start from the assumption that there is a strong WNP monsoon in JJA(0). In response to enhanced WNP monsoon heating, northward low-level cross-equatorial winds are generated. The anomalous winds enhance the seasonal mean winds, leading to increased surface evaporation and ocean vertical mixing and thus negative SSTA in the eastern IO and off the Asian coast. It is seen from Fig. 12 that the strongest SST cooling appears in the BOB, SCS, and MC. This SST cooling has a significant impact on the strength of the annual convective maximum that migrates to Southeast Asia in SON and the MC in DJF (Meehl 1987). The so-induced suppressed convection in the SCS and MC may further induce anomalous westerlies over the equatorial western Pacific through an anomalous Walker circulation.

The curl of the zonal wind stress anomaly near the equator may exert a dynamic impact on SST by exciting upwelling oceanic Rossby waves and by lifting the ocean thermocline (Masumoto and Yamagata 1991b). As a result, the ocean surface cools. Figure 13 shows the regressed SST tendency and surface wind stress fields in SON(0) and DJF(1). The negative SST tendency in the western Pacific (i.e., the blue-shaded region in Fig. 13) is indeed, to a large extent, overlapped by a strong cyclonic wind stress curl.

Figure 14 shows the relative contribution of the ocean 3D advection term versus the net heat flux term over the WNP box (10° – 15° N, 140° – 160° E) where the maximum SST tendencies appear. The major cause of the ocean surface cooling arises from ocean dynamics (i.e., 3D ocean temperature advection), while the net heat flux effect is modest, particularly in DJF(1).

The cold SSTA over the WNP, once initiated by the ocean dynamics, may persist from northern winter to the following summer through the TAS feedback proposed by Wang et al. (2000). The persistent cold SSTA eventually leads to suppressed convection and thus a weaker WNP monsoon in JJA(1), thus completing a TBO transition from a local cyclonic circulation in JJA(0) to an anticyclone in JJA(1). The weakened WNP monsoon induces southward cross-equatorial

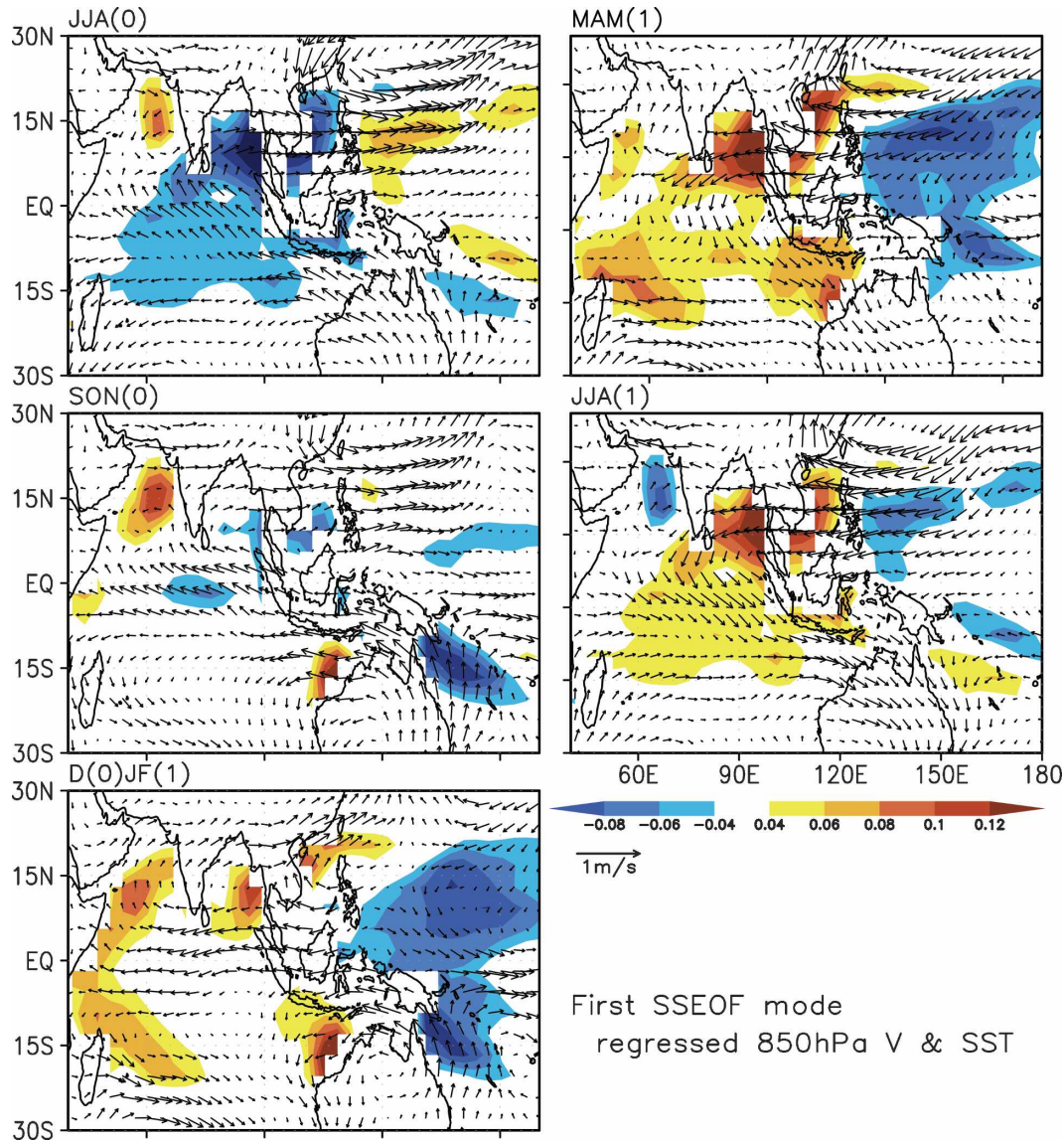


FIG. 12. Same as in Fig. 11, except for the regressed SST (shading; K) field from the hybrid coupled GCM.

flows, leading to anomalous ocean surface warming in the eastern IO and SCS and, thus, the second half of the TBO cycle begins in this region.

The scenario above illustrates a mechanism for sustaining the TBO in the monsoon–warm ocean region. The key processes involved include 1) cross-equatorial flows associated with the variability of the WNP monsoon, 2) the impact of the local SSTa on the annual convective maximum over the SCS and MC and the associated regional-scale atmospheric circulation anomaly in the western equatorial Pacific, and 3) a dynamic ocean response to the wind stress curl in the western Pacific. Note that the hybrid coupled GCM experiment above includes not only the atmosphere–

ocean interaction but also the atmosphere–land interaction. To isolate the land effect, we conducted an additional (atmosphere–land interaction only) experiment by specifying the climatological monthly mean SST in the global oceans. The diagnosis of the model output, using the same SSEO analysis procedure, reveals that no observed TBO evolution patterns appear in this case, suggesting the importance of the atmosphere–warm ocean interaction in causing the observed TBO structure and evolution in the Indo-Pacific region.

4. Connection of the TBO to ENSO

In this section we intend to demonstrate, using a second model (an intermediate coupled model), that the

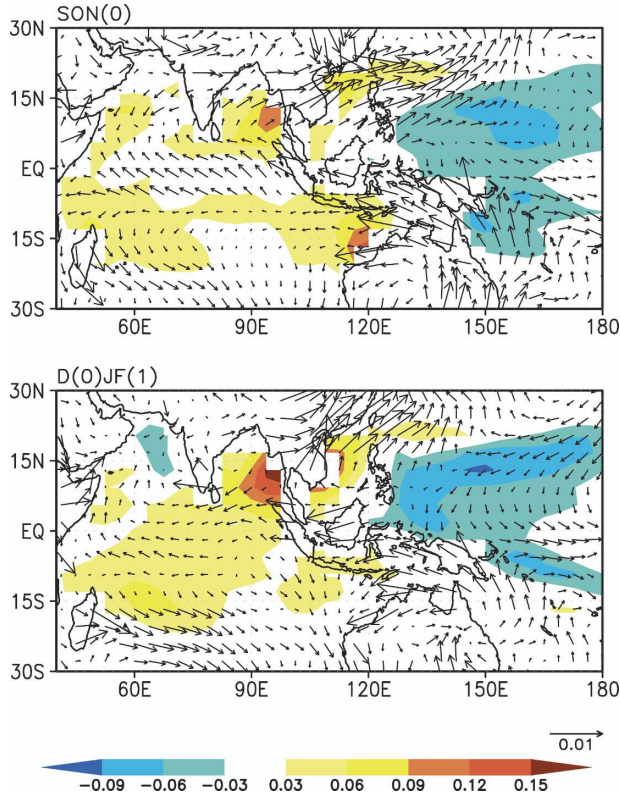


FIG. 13. The time tendency of the regressed SSTA field (shading; K season⁻¹) and surface wind stress (N m⁻²) patterns associated with the model TBO.

biennial component of ENSO could involve teleconnections across the Indo-Pacific Oceans as first suggested by Meehl (1987). To clearly demonstrate this hypothesis, we intentionally filter out the El Niño delayed oscillator dynamics (Suarez and Schopf 1988) in this model by suppressing the effects of the thermocline depth variation in SST.

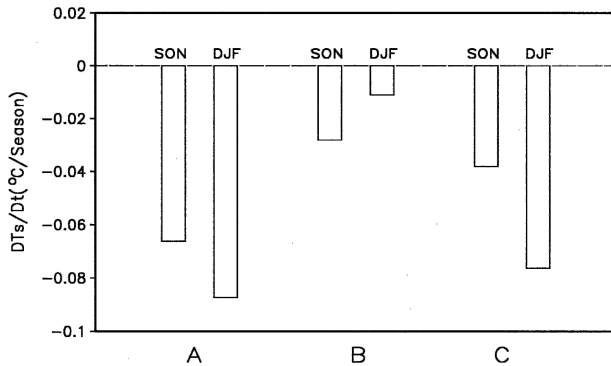


FIG. 14. SST tendency terms averaged in a western North Pacific domain (10°–15°N, 140°–160°E) in SON and DJF: (a) a local time change rate of SST, (b) a net heat flux forcing term, and (c) a 3D temperature advection term.

The coupled model covers the entire tropical Pacific and Indian Oceans. The oceanic component is similar to that of Zebiak and Cane (1987) except that in the SST equation we include the latent heat flux term but drop the vertical advection term associated with the subsurface temperature/thermocline depth variations. The anomalous SST equation may be written as

$$\frac{\partial T'}{\partial t} = -\mathbf{V} \cdot \nabla T' - \mathbf{V}' \cdot \nabla \bar{T} - w' \bar{T}_z - \frac{Q'_{LH}}{\rho C_w H},$$

where a variable with a prime represents the interannual anomaly and a variable with a bar denotes the annual cycle basic state. Here, $H = 50$ m is the mean depth of the oceanic mixed layer.

An empirical atmospheric model is used, which describes four types of anomalous wind responses to the underlying SSTA (see Fig. 15). A certain type of sur-

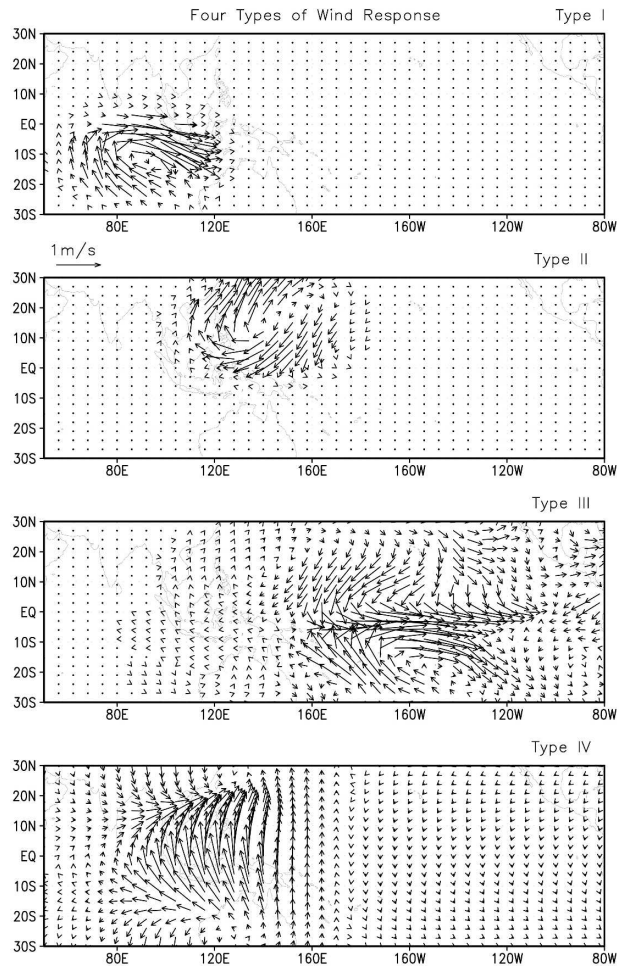


FIG. 15. Patterns of anomalous surface winds in response to the SSTA in the SEIO (5°–20°S, 90°–110°E; type I), WNP (5°–20°N, 140°–160°E; type II), CEP (10°S–10°N, 180°–100°W; type III), and anomalous heating over the WNP monsoon trough (type IV).

face wind response switches on when a defined type of SST anomaly appears in a particular region. The first three types of anomalous wind patterns (i.e., types I, II, and III) are derived based on regressions of the observed wind with the SSTA in the SEIO (5° – 20° S, 90° – 110° E), WNP (5° – 20° N, 140° – 160° E), and CEP (10° S– 10° N, 180° – 100° W), respectively. The amplitude of the wind response is defined to be a unit value (i.e., 1 m s^{-1}), which corresponds to a box-averaged SSTA of $+0.4 \text{ K}$ in the SEIO, -0.3 K in the WNP, and $+1.0 \text{ K}$ in the CEP. The type IV wind pattern is derived from the Gill (1980) model solution in response to an antisymmetric heat source, to mimic the cross-equatorial flow response to enhanced (or weakened) heating over the WNP monsoon trough. This type of the wind response is switched on only in boreal summer when the WNP SST is anomalously warm (or cold). In addition, the model describes an equatorial wind response to anomalous MC heating, with the use of the type III wind pattern within the equatorial zone (i.e., 5° S– 5° N). The strength of the wind response depends on the SSTA in the SEIO based on the fact that a cold SSTA off Sumatra is often associated with the suppressed convection in the MC (possibly due to the induced wind divergence and reduction of moisture as well as the local Walker circulation). A cold SSTA of -0.5°C in the SEIO corresponds to a westerly wind anomaly of 1 m s^{-1} in the central equatorial Pacific.

The coupled model is integrated for 10 yr. An oscillatory solution with a period of 2 yr emerges in a reasonable parameter regime. Figure 16 shows the time evolution of the SSTA averaged in the SEIO, WNP, and CEP boxes. The SSTAs in all three regions show a pronounced TBO with reasonable amplitudes.

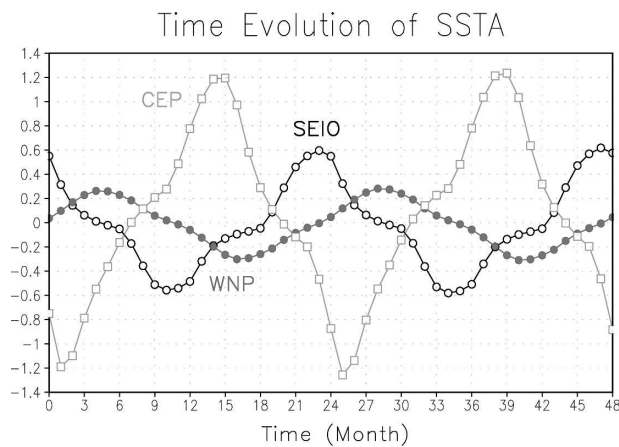


FIG. 16. Time evolution of the SSTA (K) in the WNP (closed circle), SEIO (open circle), and CEP (square) simulated by an intermediate coupled model that does not include the delayed oscillator dynamics.

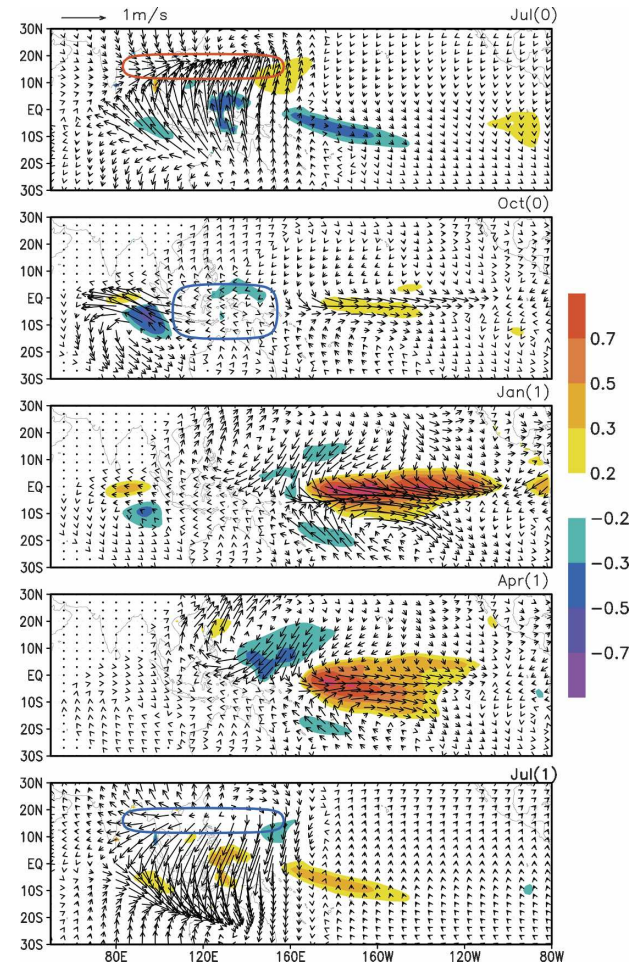


FIG. 17. Seasonal evolution of the model SSTA (shaded; K) and surface wind anomaly (vector) from July of year 0 to July of year 1. The red (blue) solid line represents positive (negative) atmospheric heating anomalies over the western Pacific monsoon trough or over the Maritime Continent.

A significant SST variation (with an amplitude of 1.4°C) appears in the CEP. Note that this SST variation is not attributed to the delayed oscillator dynamics, but instead to an interbasin teleconnection between the tropical IO and Pacific. The mechanism through which the TBO of the Niño-3 SSTA is generated is summarized as follows. To aid the discussion, the seasonal evolution of the model SST and wind fields is illustrated in Fig. 17. Starting from the boreal summer (July) of year 0 when the WNP monsoon is strong (in response to local warm SSTA), the enhanced WNP monsoon leads to anomalous northward cross-equatorial flows. The along-coast wind leads to a strong local SST cooling off of Sumatra (due to enhanced evaporation, vertical mixing, and coastal upwelling). The cold SSTA off of Sumatra leads to the development of an anticyclonic circulation anomaly near the surface, which further en-

TABLE 1. Major processes involved with the TBO in the Indo-Pacific warm ocean region.

JJA(0)	Initiation of a cold SSTA in the SEIO due to anomalous northward cross-equatorial winds associated with enhanced WNP monsoon heating; rapid development of the cold SSTA through local positive air–sea feedback
SON(0)	The local air–sea feedback leads to mature phase of the SEIO SSTA that further leads to suppression of convection in the MC and an anomalous Walker circulation over the equatorial Pacific
D(0)JF(1)	Initiation and development of a warm SSTA in the CEP; atmospheric Rossby wave response to the anomalous CEP heat source leads to a cold SSTA and anomalous anticyclonic circulation in the WNP
MAM(1)	The TAS feedback maintains the anomalous SST and anticyclonic circulation in the WNP
JJA(1)	The cold SSTA eventually leads to a weak WNP monsoon, which induces anomalous southward cross-equatorial flows and initiates a warm SSTA in the SEIO

hances the cooling because the mean wind is southeasterly. This positive feedback eventually leads to a mature phase of the anticyclone and SST anomalies in northern fall. In boreal winter, because of the change of the seasonal wind, this positive feedback diminishes (Li et al. 2003). The convection/SST variability in the SEIO is closely associated with that in the western IO, through the effect of westward-propagating oceanic Rossby waves (Webster et al. 1999) and/or the thermocline–SST–wind feedback (Li et al. 2003). Thus, the development of the Indian Ocean dipole is a part of the seasonally evolving TBO (Loschnigg et al. 2003; Meehl et al. 2003).

The surface cooling off of Sumatra and the associated local Walker circulation over the IO lead to boundary layer moisture divergence and suppression of convection over the MC in northern fall. The suppressed convection further induces an anomalous westerly in the CEP (Krishnamurti 1971; Stone and Chervin 1984; Chang and Li 2001). The westerly anomaly leads to the CEP warming through reduced surface evaporation/vertical mixing and anomalous downwelling, and the warming in turn enhances the westerly. As a result of this positive feedback, the SSTA in the CEP grows. Meanwhile off-equatorial winds (due to the Rossby wave response to the central Pacific heating) induce a cooling in the WNP (because of the mean northeasterly in DJF). The cooling, through its feedback with a local anomalous anticyclone (Wang et al. 2000), persists from boreal winter to the subsequent summer, leading to a weak WNP monsoon in July(1).

Table 1 summarizes the major processes involved in the interbasin teleconnection. It consists of the following three types of “atmospheric bridges” that link the tropical Indian Ocean to the Pacific Ocean:

- a north–south teleconnection that connects the WNP monsoon and SSTA in the SEIO through anomalous cross-equatorial winds;
- an east–west teleconnection that connects the SEIO and CEP through anomalous convective heating over the MC; and

- an El Niño–WNP teleconnection that connects the equatorial eastern Pacific SSTA and the WNP monsoon through atmospheric Rossby wave responses to anomalous heating in the central Pacific and the TAS feedback that maintains the WNP anomalies from northern winter to the following summer.

The coupled experiment above suggests that given correct atmospheric responses to particular SSTA patterns, the TBO can be generated through a teleconnection between the tropical IO and Pacific, without the explicit involvement of the delayed oscillator dynamics. Both the Indian Ocean dipole and the biennial component of the ENSO are parts of the TBO.

5. Conclusions

Using a season-sequence EOF analysis approach, we reveal the structure and seasonal evolutionary characteristics of the observed TBO in the warm Indo-Pacific ocean region. It is noted that major convective activity centers associated with the TBO in the region reside in the SEIO and WNP. Accompanying the TBO convection centers are two large-scale anticyclonic (or cyclonic) circulation patterns. The circulation anomalies have a first-baroclinic-mode vertical structure. The life cycle and evolution of the two anticyclonic (or cyclonic) flow anomalies in the SEIO and WNP are remarkably different. Whereas the anomaly in the SEIO is initiated in northern summer and reaches a peak phase in northern fall, the circulation anomaly in the WNP is initiated in northern fall and persists for two to three seasons till the subsequent summer, and has a significant impact on the WNP summer monsoon. Associated with the convection and circulation evolution in the monsoon–warm ocean region, the SSTA in the CEP persists from northern summer until winter, reaching a peak phase in northern fall. This TBO evolution differs from the El Niño life cycle, which has a peak phase in DJF.

The TBO mechanisms in the warm ocean region are investigated using two models. The first is a hybrid coupled GCM in which atmosphere and ocean are fully

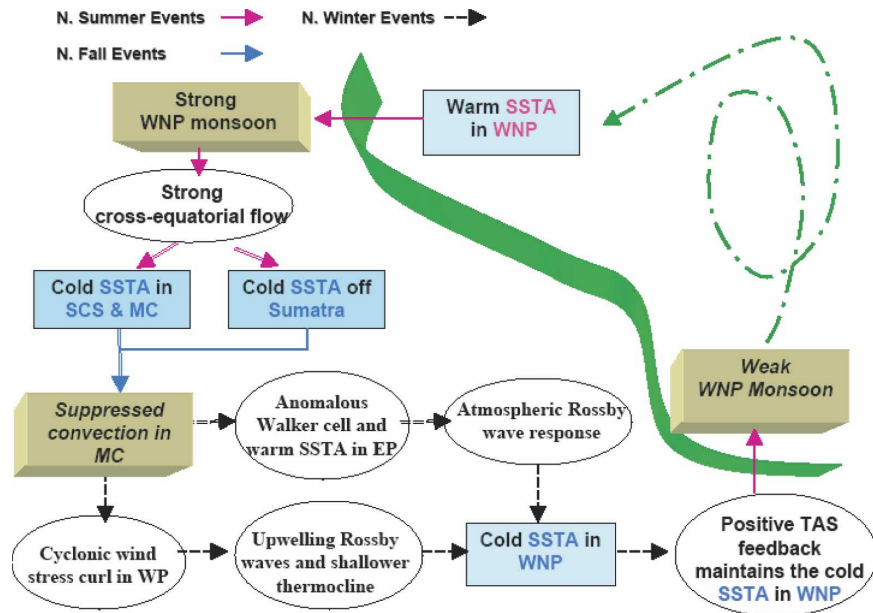


FIG. 18. A schematic diagram illustrating essential processes that lead to the TBO in the tropical Pacific and Indian Oceans. The left part of a green ribbon consists of a half of the TBO cycle, which starts from a strong WNP summer monsoon at year 0 and ends to a weak monsoon at year 1. The red, blue, and black arrows indicate, respectively, northern summer, fall, and winter events.

interactive only in the tropical western Pacific and Indian Oceans. A seasonally evolving TBO pattern similar to the observed appears in the model, even though El Niño forcing is not included. The numerical experiment clearly demonstrates the importance of the atmosphere–warm ocean interaction in causing the TBO.

The connections between the TBO and ENSO are further studied in a second model that explicitly excludes the delayed oscillator dynamics. The TBO in the eastern Pacific SST in the model is produced by teleconnections between the tropical Pacific and Indian Oceans. The teleconnections consist of three branches or “atmospheric bridges.” The first one is a north–south teleconnection between the anomalous monsoon in the WNP and the SSTA in the SEIO (Li et al. 2002). The key process involved in this teleconnection is the anomalous Hadley circulation and associated cross-equatorial flows. The second is a east–west teleconnection between convection/circulation anomalies in the IO and SSTA in the CEP. It involves a two-way interaction. On one hand, the CEP SSTA may remotely impact the IO wind through an anomalous Walker circulation (Meehl 1987; Murtugudde et al. 2000; Annamalai and Liu 2005). On the other hand, the IO SSTA may remotely influence the CEP through the modulation of convection over the MC (Yu et al. 2002; Watanabe and Jin 2002; Ashok et al. 2003) and, thus,

onward to the Pacific through large-scale east–west circulations in the atmosphere. The third is the El Niño–WNP monsoon teleconnection that connects the CEP SSTA and the WNP monsoon through an atmospheric Rossby wave response and the TAS feedback (Wang et al. 2000).

Different from Chang and Li (2000), which emphasizes the effect of the Indian and Australian monsoons on the TBO, the current study points out a complementary scenario in which the transition of the WNP monsoon, from a strong to a weak year, plays a key role. Both scenarios complement each other as the TBO combines different processes. For example, the south Asian monsoon, noted to play a key role in the TBO in earlier studies, is also connected to the tropical Pacific through the large-scale east–west atmospheric circulation noted here, and is consistent with the regional mechanisms documented in the present paper.

Figure 18 is a flowchart that combines the physical processes from both the hybrid coupled GCM and intermediate coupled model experiments together in a unified framework. Starting from a strong WNP monsoon in boreal summer, the strong convection in the WNP causes strong northward cross-equatorial flows. The anomalous winds induce cold SSTAs in the SCS, MC, and SEIO off Sumatra, leading to suppressed convection in the MC through either a local SSTA impact

on the seasonal convective maximum or its effect on the surface divergence and local Walker circulation over the IO. The suppressed convection in the MC induces anomalous westerlies in the western Pacific, which lead to a cold SSTA in the WNP through either a direct ocean dynamic effect (via upwelling ocean Rossby waves and the associated thermocline changes) or an indirect atmospheric effect (through the CEP heating and the associated atmospheric Rossby wave response). The so-induced cold SSTA in the WNP persists through the TAS feedback and leads to the weakening of the WNP monsoon in the following summer. Thus, the second half cycle of the TBO begins. The numerical experiments confirm earlier hypotheses that the biennial component of ENSO is a part of TBO (Meehl et al. 2003), resulting from teleconnections between the tropical Pacific and Indian Oceans.

Acknowledgments. This work was supported by NSF Grant ATM01-19490, by DOD/ONR Grant N000140310739, and by the Japan Agency for Marine–Earth Science and Technology (JAMSTEC) through its sponsorship of the International Pacific Research Center. The authors acknowledge Dr. Q. Zhang for a preliminary analysis of the hybrid coupled GCM. Portions of this study were supported by the Office of Biological and Environmental Research, U.S. Department of Energy, as part of its Climate Change Prediction Program, and the National Center for Atmospheric Research.

REFERENCES

- Annamalai, H., and P. Liu, 2005: Response of the Asian summer monsoon to changes in ENSO properties. *Quart. J. Roy. Meteor. Soc.*, **131**, 805–831.
- Ashok, K., Z. Guan, and T. Yamagata, 2003: A look at the relationship between the ENSO and the Indian Ocean dipole. *J. Meteor. Soc. Japan*, **81**, 41–56.
- Barnett, T. P., 1991: The interaction of multiple time scales in the tropical climate system. *J. Climate*, **4**, 269–285.
- Brinkop, S., and E. Roeckner, 1995: Sensitivity of a general circulation model to parameterizations of cloud–turbulence interactions in the atmospheric boundary layer. *Tellus*, **47A**, 197–220.
- Chambers, D. P., B. D. Tapley, and R. H. Stewart, 1999: Anomalous warming in the Indian Ocean coincident with El Niño. *J. Geophys. Res.*, **104**, 523–533.
- Chang, C.-P., and T. Li, 2000: A theory of the tropical tropospheric biennial oscillation. *J. Atmos. Sci.*, **57**, 2209–2224.
- , and —, 2001: Tropical tropospheric biennial oscillation and ENSO. *East Asian and Western Pacific Meteorology and Climate*, C.-P. Chang et al., Eds., Book Series on East Asian Meteorology, Vol. 1, World Scientific, 167–179.
- , Y. Zhang, and T. Li, 2000a: Interannual and interdecadal variations of the East Asian summer monsoon and tropical Pacific SSTs. Part I: Roles of the subtropical ridge. *J. Climate*, **13**, 4310–4325.
- , —, and —, 2000b: Interannual and interdecadal variations of the East Asian summer monsoon and tropical Pacific SSTs. Part II: Meridional structure of the monsoon. *J. Climate*, **13**, 4326–4340.
- , P. A. Harr, and J. Ju, 2001: Possible role of Atlantic circulation on the weakening Indian monsoon rainfall–ENSO relationship. *J. Climate*, **14**, 2376–2380.
- Chen, T.-C., S.-Y. Wang, W.-R. Huang, and M.-C. Yen, 2004: Variation of the East Asian summer monsoon rainfall. *J. Climate*, **17**, 744–762.
- Christiano, L. J., and T. J. Fitzgerald, 2003: The band pass filter. *Int. Econ. Rev.*, **44**, 435–465.
- Chung, C., and S. Nigam, 1999: Asian summer monsoon–ENSO feedback on the Cane–Zebiak model ENSO. *J. Climate*, **12**, 2787–2807.
- Clarke, A. J., and L. Shu, 2000: Quasi-biennial winds in the far western equatorial Pacific phase-locking El Niño to the seasonal cycle. *Geophys. Res. Lett.*, **27**, 771–774.
- , X. Liu, and S. Van Gorder, 1998: Dynamics of the biennial oscillation in the equatorial Indian and far western Pacific Oceans. *J. Climate*, **11**, 987–1001.
- Dumenil, L., and E. Todini, 1992: A rainfall–runoff scheme for use in the Hamburg climate model. *Advances in Theoretical Hydrology—A Tribute to James Dooge*, J. P. O’Kane, Ed., European Geophysical Society Series on Hydrological Sciences, Vol. 1, Elsevier Press, 129–157.
- Fouquart, Y., and B. Bonnel, 1989: Computations of solar heating of the earth’s atmosphere: A new parameterization. *Beitr. Phys. Atmos.*, **53**, 35–62.
- Fu, X., and B. Wang, 2001: A coupled modeling study of the annual cycle of the Pacific cold tongue. Part I: Simulation and sensitivity experiments. *J. Climate*, **14**, 765–779.
- , —, and T. Li, 2002: Impacts of air–sea coupling on the simulation of the mean Asian summer monsoon in the ECHAM4 model. *Mon. Wea. Rev.*, **130**, 2889–2904.
- , —, —, and J. McCreary, 2003: Coupling between northward propagating ISO and SST in the Indian Ocean. *J. Atmos. Sci.*, **60**, 1733–1753.
- Gaspar, P., 1988: Modeling the seasonal cycle of the upper ocean. *J. Phys. Oceanogr.*, **18**, 161–180.
- Gill, A. E., 1980: Some simple solutions for heat-induced tropical circulation. *Quart. J. Roy. Meteor. Soc.*, **106**, 447–462.
- Hendon, H. H., 2003: Indonesian rainfall variability: Impacts of ENSO and local air–sea interaction. *J. Climate*, **16**, 1775–1790.
- Ju, J., and J. M. Slingo, 1995: The Asian summer monsoon and ENSO. *Quart. J. Roy. Meteor. Soc.*, **121**, 1133–1168.
- Kalnay, E., and Coauthors, 1996: The NCEP/NCAR 40-Year Reanalysis Project. *Bull. Amer. Meteor. Soc.*, **77**, 437–471.
- Kim, K. M., and K. M. Lau, 2001: Dynamics of monsoon-induced biennial variability in ENSO. *Geophys. Res. Lett.*, **28**, 315–318.
- Krishnamurti, T. N., 1971: Tropical east–west circulation during the northern summer. *J. Atmos. Sci.*, **28**, 1342–1347.
- Kumar, K. K., B. Rajagopalan, and M. C. Cane, 1999: On the weakening relationship between the Indian monsoon and ENSO. *Science*, **284**, 2156–2159.
- Lau, K. M., 2001: Monsoon–ENSO relationship: A new paradigm. *Dynamics of Atmospheric and Oceanic Circulations and Climate*, M. Wang et al., Eds., China Meteorological Press, 533–551.
- , and P. Sheu, 1988: Annual cycle, QBO and Southern Oscil-

- lation in global precipitation. *J. Geophys. Res.*, **93**, 10 975–10 988.
- , and S. Yang, 1996: The Asian monsoon and predictability of the tropical ocean atmosphere system. *Quart. J. Roy. Meteor. Soc.*, **122**, 945–957.
- , and H. T. Wu, 2001: Principal modes of coupled rainfall–SST variability for the Asian summer monsoon: A reassessment of the monsoon–ENSO relationship. *J. Climate*, **14**, 2880–2895.
- , K. M. Kim, and S. Yang, 2000: Dynamic and boundary forcing characteristics of regional components of the Asian summer monsoon. *J. Climate*, **13**, 2461–2482.
- Lau, N.-C., and M. J. Nath, 2000: Impacts of ENSO on the variability of the Asian–Australian monsoons as simulated in GCM experiments. *J. Climate*, **13**, 4287–4309.
- Li, T., and Y. S. Zhang, 2002: Processes that determine the quasi-biennial and lower-frequency variability of the south Asian monsoon. *J. Meteor. Soc. Japan*, **80**, 1149–1163.
- , and B. Wang, 2005: A review on the western North Pacific monsoon: Synoptic-to-interannual variabilities. *Terr. Atmos. Ocean Sci.*, **16**, 285–314.
- , C.-W. Tham, and C.-P. Chang, 2001a: A coupled air–sea–monsoon oscillator for the tropospheric biennial oscillation. *J. Climate*, **14**, 752–764.
- , B. Wang, and C.-P. Chang, 2001b: Theories on the tropospheric biennial oscillation: A review. *Dynamics of Atmospheric and Oceanic Circulations and Climate*, M. Wang et al., Eds., China Meteorological Press, 252–276.
- , Y. S. Zhang, C. P. Chang, and B. Wang, 2001c: On the relationship between Indian Ocean SST and Asian summer monsoon. *Geophys. Res. Lett.*, **28**, 2843–2846.
- , Y. S. Zhang, E. Lu, and D. Wang, 2002: Relative role of dynamic and thermodynamic processes in the development of the Indian Ocean dipole. *Geophys. Res. Lett.*, **29**, 2110–2113.
- , B. Wang, C.-P. Chang, and Y. Zhang, 2003: A theory for the Indian Ocean dipole–zonal mode. *J. Atmos. Sci.*, **60**, 2119–2135.
- , Y.-C. Tung, and J.-W. Hwu, 2005: Remote and local SST forcing in shaping Asian–Australian monsoon anomalies. *J. Meteor. Soc. Japan*, **83**, 153–167.
- Loschnigg, J., G. A. Meehl, P. J. Webster, J. M. Arblaster, and G. P. Compo, 2003: The Asian monsoon, the tropospheric biennial oscillation, and the Indian Ocean dipole in the NCAR CSM. *J. Climate*, **16**, 2138–2158.
- Louis, J. F., 1979: A parametric model of vertical eddy fluxes in the atmosphere. *Bound.-Layer Meteor.*, **17**, 187–202.
- Masumoto, Y., and T. Yamagata, 1991a: On the origin of a model ENSO in the western Pacific. *J. Meteor. Soc. Japan*, **69**, 197–207.
- , and —, 1991b: Response of the western tropical Pacific to the Asian winter monsoon: The generation of the Mindanao Dome. *J. Phys. Oceanogr.*, **21**, 1386–1398.
- McCreary, J. P., and Z. J. Yu, 1992: Equatorial dynamics in a 2.5-layer model. *Progress in Oceanography*, Vol. 29, Pergamon, 61–132.
- Meehl, G. A., 1987: The annual cycle and interannual variability in the tropical Pacific and Indian Ocean region. *Mon. Wea. Rev.*, **115**, 27–50.
- , 1993: A coupled air–sea biennial mechanism in the tropical Indian and Pacific regions: Role of the ocean. *J. Climate*, **6**, 31–41.
- , 1994: Coupled land–ocean–atmosphere processes and south Asian monsoon variability. *Science*, **266**, 263–267.
- , 1997: The south Asian monsoon and the tropospheric biennial oscillation. *J. Climate*, **10**, 1921–1943.
- , and J. M. Arblaster, 2002a: GCM sensitivity experiments for the Indian monsoon and tropospheric biennial oscillation transition conditions. *J. Climate*, **15**, 923–944.
- , and —, 2002b: The tropospheric biennial oscillation and Asian–Australian monsoon rainfall. *J. Climate*, **15**, 722–744.
- , —, and J. Loschnigg, 2003: Coupled ocean–atmosphere dynamical processes in the tropical Indian and Pacific Ocean regions and the TBO. *J. Climate*, **16**, 2138–2158.
- Mooley, D. A., and B. Parthasarathy, 1984: Fluctuations in all-India summer monsoon rainfall during 1871–1978. *Climatic Change*, **6**, 287–301.
- Morcrette, J.-J., L. Smith, and Y. Fouquart, 1986: Pressure and temperature dependence of the absorption in longwave radiation parameterizations. *Beitr. Phys. Atmos.*, **59**, 455–469.
- Murtugudde, R., J. P. McCreary Jr., and A. J. Busalacchi, 2000: Oceanic processes associated with anomalous events in the Indian Ocean with relevance to 1997–1998. *J. Geophys. Res.*, **105**, 3295–3306.
- Nicholls, N., 1978: Air–sea interaction and the quasi-biennial oscillation. *Mon. Wea. Rev.*, **106**, 1505–1508.
- Nordeng, T. E., 1996: Extended versions of the convective parameterization scheme at ECMWF and their impact on the mean and transient activity of the model in the tropics. Research Dept. Tech. Memo. 206, ECMWF, Reading, United Kingdom, 41 pp.
- Ogasawara, N., A. Kitoh, T. Yasunari, and A. Noda, 1999: Tropospheric biennial oscillation of the ENSO–monsoon system in the MRI coupled GCM. *J. Meteor. Soc. Japan*, **77**, 1247–1270.
- Rasmusson, E. M., and T. H. Carpenter, 1983: The relationship between eastern equatorial Pacific sea surface temperatures and rainfall over India and Sri Lanka. *Mon. Wea. Rev.*, **111**, 517–528.
- , X.-L. Wang, and C. F. Ropelewski, 1990: The biennial component of ENSO variability. *J. Mar. Syst.*, **1**, 71–96.
- Reason, C. J. C., R. J. Allan, J. A. Lindsay, and T. J. Ansell, 2000: ENSO and climatic signals across the Indian Ocean basin in the global context: Part I. Interannual composite patterns. *Int. J. Climatol.*, **20**, 1285–1327.
- Rockel, B., E. Raschke, and B. Weyres, 1991: A parameterization of broad band radiative transfer properties of water, ice and mixed clouds. *Beitr. Phys. Atmos.*, **64**, 1–12.
- Roeckner, E., and Coauthors, 1996: The atmospheric general circulation model ECHAM-4: Model description and simulation of present-day climate. Max Planck Institute for Meteorology Rep. 218, Hamburg, Germany, 90 pp.
- Ropelewski, C. F., M. S. Halpert, and X. Wang, 1992: Observed tropospheric biennial variability and its relationship to the Southern Oscillation. *J. Climate*, **5**, 594–614.
- Saji, N. H., B. N. Goswami, P. N. Vinayachandran, and T. Yamagata, 1999: A dipole mode in the tropical Indian Ocean. *Nature*, **401**, 360–363.
- Shen, S., and K.-M. Lau, 1995: Biennial oscillation associated with the East Asian summer monsoon and tropical Pacific sea surface temperatures. *J. Meteor. Soc. Japan*, **73**, 105–124.
- Shukla, J., and D. A. Paolino, 1983: The Southern Oscillation and long-range forecasting of the summer monsoon rainfall over India. *Mon. Wea. Rev.*, **111**, 1830–1837.
- Slingo, J. M., and H. Annamalai, 2000: 1997: The El Niño of the

- century and the response of the Indian summer monsoon. *Mon. Wea. Rev.*, **128**, 1778–1797.
- Stone, P. H., and R. M. Chervin, 1984: Influence of ocean surface temperature gradient and continentality on the Walker Circulation. Part II: Prescribed global changes. *Mon. Wea. Rev.*, **112**, 1524–1534.
- Suarez, M. J., and P. S. Schopf, 1988: A delayed action oscillator for ENSO. *J. Atmos. Sci.*, **45**, 3283–3287.
- Tian, S. F., and T. Yasunari, 1992: Time and space structure of interannual variations in summer rainfall over China. *J. Meteor. Soc. Japan*, **70**, 585–596.
- Tiedtke, M., 1989: A comprehensive mass flux scheme for cumulus parameterization in large-scale models. *Mon. Wea. Rev.*, **117**, 1779–1800.
- Tomita, T., and T. Yasunari, 1996: Role of the northeast winter monsoon on the biennial oscillation of the ENSO/monsoon system. *J. Meteor. Soc. Japan*, **74**, 399–413.
- Wainer, I., and P. J. Webster, 1996: Monsoon–ENSO interaction using a simple coupled ocean–atmosphere model. *J. Geophys. Res.*, **101**, 25 599–25 614.
- Wang, B., and Q. Zhang, 2002: Pacific–East Asian teleconnection. Part II: How the Philippine Sea anticyclone is established during development of El Niño. *J. Climate*, **15**, 3252–3265.
- , and T. Li, 2004: East Asian monsoon–ENSO interactions. *East Asian and Western Pacific Meteorology and Climate*, C.-P. Chang et al., Eds., Book Series on East Asian Meteorology, Vol. 2, World Scientific, 177–212.
- , —, and P. Chang, 1995: An intermediate model of the tropical Pacific ocean. *J. Phys. Oceanogr.*, **25**, 1599–1616.
- , R. Wu, and X. Fu, 2000: Pacific–East Asian teleconnection: How does ENSO affect East Asian climate? *J. Climate*, **13**, 1517–1536.
- , —, and T. Li, 2003: Atmosphere–warm ocean interaction and its impact on Asian–Australian monsoon variation. *J. Climate*, **16**, 1195–1211.
- Wang, C., R. H. Weisberg, and J. I. Virmani, 1999: Western Pacific interannual variability associated with the El Niño–Southern Oscillation. *J. Geophys. Res.*, **104**, 5131–5149.
- Wang, W., S. Saha, H. Pan, S. Nadiga, and G. White, 2005: Simulation of ENSO in the new NCEP Coupled Forecast System Model (CFS03). *Mon. Wea. Rev.*, **133**, 1574–1593.
- Watanabe, M., and F.-F. Jin, 2002: Role of Indian Ocean warming in the development of Philippine Sea anticyclone during ENSO. *Geophys. Res. Lett.*, **29**, 1478, doi:10.1029/2001GL014318.
- Webster, P. J., and S. Yang, 1992: Monsoon and ENSO: Selectively interactive systems. *Quart. Roy. J. Meteor. Soc.*, **118**, 877–926.
- , V. O. Magana, T. N. Palmer, J. Shukla, R. A. Tomas, M. Yanai, and T. Yasunari, 1998: Monsoons: Processes, predictability, and the prospects for prediction. *J. Geophys. Res.*, **103**, 14 451–14 510.
- , A. M. Moore, J. P. Loschnigg, and R. R. Leben, 1999: Coupled ocean–atmosphere dynamics in the Indian Ocean during 1997–98. *Nature*, **401**, 356–360.
- Xie, P., and P. A. Arkin, 1997: Global precipitation: A 17-year monthly analysis based on gauge observations, satellite estimates, and numerical outputs. *Bull. Amer. Meteor. Soc.*, **78**, 2539–2558.
- Yanai, M., and C. Li, 1994: Interannual variability of Asian summer monsoon and its relationship with ENSO, Eurasian snow cover and heating. *Proc. Int. Conf. on Monsoon Variability and Prediction*, Vol. 1, WMO/TD 619, Trieste, Italy, International Center for Theoretical Physics, 27–34.
- Yang, S., and K.-M. Lau, 1998: Influences of sea surface temperature and ground wetness on Asian summer monsoon. *J. Climate*, **11**, 3230–3246.
- Yasunari, T., 1990: Impact of the Indian monsoon on the coupled atmosphere/ocean system in the tropical Pacific. *Meteor. Atmos. Phys.*, **44**, 29–41.
- , 1991: The monsoon year—A new concept of the climate year in the tropics. *Bull. Amer. Meteor. Soc.*, **72**, 1331–1338.
- , and R. Suppiah, 1988: Some problems on the interannual variability of Indonesian monsoon rainfall. *Tropical Rainfall Measurements*, J. S. Theon and N. Fugono, Eds., Deepak Publishing, 113–122.
- Yu, J.-Y., C. R. Mechoso, A. Arakawa, and J. C. Williams, 2002: Impacts of the Indian Ocean on the ENSO cycle. *Geophys. Res. Lett.*, **29**, 1204, doi:10.1029/2001GL014098.
- Zebiak, S. E., and M. A. Cane, 1987: A model El Niño–Southern Oscillation. *Mon. Wea. Rev.*, **115**, 2262–2278.